

Control of polarization and dipole moment in low-dimensional semiconductor nanostructures

L. H. Li, M. Mexis, P. Ridha, M. Bozkurt, G. Patriarche et al.

Citation: *Appl. Phys. Lett.* **95**, 221116 (2009); doi: 10.1063/1.3269592

View online: <http://dx.doi.org/10.1063/1.3269592>

View Table of Contents: <http://apl.aip.org/resource/1/APPLAB/v95/i22>

Published by the [American Institute of Physics](#).

Related Articles

Modification of the conduction band edge energy via hybridization in quantum dots

Appl. Phys. Lett. **101**, 193104 (2012)

Photoluminescence and light reabsorption in SiC quantum dots embedded in binary-polyelectrolyte solid matrix

J. Appl. Phys. **112**, 094315 (2012)

Third harmonic generation in intraband transitions of spherical silicon quantum dots

J. Appl. Phys. **112**, 094306 (2012)

Photoluminescence under high-electric field of PbS quantum dots

AIP Advances **2**, 042132 (2012)

Effect of dimensionality and morphology on polarized photoluminescence in quantum dot-chain structures

J. Appl. Phys. **112**, 084314 (2012)

Additional information on *Appl. Phys. Lett.*

Journal Homepage: <http://apl.aip.org/>

Journal Information: http://apl.aip.org/about/about_the_journal

Top downloads: http://apl.aip.org/features/most_downloaded

Information for Authors: <http://apl.aip.org/authors>

ADVERTISEMENT



Goodfellow
metals • ceramics • polymers • composites
70,000 products
450 different materials
small quantities fast

www.goodfellowusa.com

Control of polarization and dipole moment in low-dimensional semiconductor nanostructures

L. H. Li (李联合),^{1,a)} M. Mexis,² P. Ridha,¹ M. Bozkurt,³ G. Patriarache,⁴ P. M. Smowton,² P. Blood,² P. M. Koenraad,³ and A. Fiore^{1,3}

¹*Ecole Polytechnique Fédérale de Lausanne, Institute of Photonics and Quantum Electronics, Station 3, CH-1015 Lausanne, Switzerland*

²*Cardiff University, The Parade, Cardiff CF24 3AA, United Kingdom*

³*COBRA Research Institute, Eindhoven University of Technology, P.O. Box 513, 5600 MB Eindhoven, The Netherlands*

⁴*LPN/CNRS, Route de Nozay, 91460 Marcoussis, France*

(Received 15 September 2009; accepted 9 November 2009; published online 4 December 2009)

We demonstrate the control of polarization and dipole moment in semiconductor nanostructures, through nanoscale engineering of shape and composition. Rodlike nanostructures, elongated along the growth direction, are obtained by molecular beam epitaxial growth. By varying the aspect ratio and compositional contrast between the rod and the surrounding matrix, we rotate the polarization of the dominant interband transition from transverse-electric to transverse-magnetic, and modify the dipole moment producing a radical change in the voltage dependence of absorption spectra. This opens the way to the optimization of quantum dot amplifiers and electro-optical modulators. © 2009 American Institute of Physics. [doi:10.1063/1.3269592]

The control of the electronic and optical properties of semiconductor nanostructures is a formidable challenge, with major impact on practical applications of nanophotonics. While high-performance lasers, amplifiers, modulators, and detectors, as well as single-photon sources, have been obtained using epitaxial quantum dots (QDs), the Stranski–Krastanow (SK) growth method typically used offers little control over the QD shape and composition profile. This lack of control has a direct influence on two key macroscopic parameters; polarization and dipole moment. Indeed, SK QDs typically have a flat shape. This results in an asymmetric potential profile and in compressive strain, which both push states with large light-hole component away from the band-edge, producing a strongly in-plane polarized ground-state transition.^{1,2} This prevents the application of QDs in in-line semiconductor optical amplifiers (SOAs), where polarization insensitivity is needed. Moreover, the In composition profile along the growth direction, resulting from the complex interplay of nucleation and In segregation, determines the spatial localization of electrons and holes, and thus the dipole moment, which is a key parameter for application in electro-optical modulators. Dipole moments oriented both parallel and antiparallel to the growth direction have been observed in different types of QDs,^{3,4} but without a clear correlation to the structural properties and thus with no possibility of control.

A better possibility of control of the vertical composition profile exists in columnar quantum dots (CQDs),⁵ obtained by depositing a short-period GaAs/InAs superlattice (SL) on top of a seed QD layer. Selective adatom incorporation in the strained areas on top of seed QDs results in a tall, In-rich column within an InGaAs matrix. The CQD height, and the In profile along the growth direction can then be controlled by the GaAs and InAs layer thickness of the SL. While ear-

lier generations of CQDs presented an approximately cubic shape, recent growth optimization has allowed the increase of the QD aspect ratio (height/diameter) >1 .^{6–9} The obtained nanostructures are more similar to quantum rods¹⁰ than to conventional QDs. The polarization of emission and gain from CQDs has been shown to gradually evolve from transverse-electric (TE) to transverse-magnetic (TM) as the height is increased^{11–14} but so far TM gain in SOAs has been obtained only in the InAs/InP system,¹⁵ where strain compensation in the barriers can be used to control the strain in the QDs. Evidence of modified dipole moment in compressive strain CQDs was also reported.¹⁶ In this letter, we report the electro-optical properties of a recent generation of InAs/GaAs CQDs with much increased aspect ratio and compositional contrast, leading to TM-dominant gain and lasing, and a radical change in the dipole moment and electroabsorption characteristics.

The CQDs were grown by molecular-beam epitaxy on GaAs (001) substrates, with the following growth sequence.^{8,9} A 1.8 monolayer (ML) InAs QD seed layer is first deposited, followed by a N -periods GaAs/InAs SL (thicknesses d_{GaAs} and d_{InAs} , respectively). The growth rates of GaAs and InAs were 0.7 and 0.1 M L/s, and the growth temperature was 500 °C. After growth of each InAs layer, a growth interruption of 5 s was applied in order to make the CQD size distribution more uniform. The In contents x_{CQD} and $x_{2\text{D}}$ in the CQD and two-dimensional (2D) layer are determined by the InAs and GaAs thicknesses (d_{InAs} and d_{GaAs}) in the SL, and by the CQD formation process. We recently reported¹⁷ that d_{InAs} and d_{GaAs} can be varied in a narrow parameter space to control the compositions, while keeping a uniform CQD with high radiative quality. In particular, we are able to controllably tune $x_{2\text{D}}$ in the 12%–16% range by varying d_{InAs} (d_{GaAs}) in the 0.62–0.95 (3–6) MLs range, while keeping x_{CQD} nearly constant. This control of $x_{2\text{D}}$ in turn allows us to extend the rod height up to at least 70 nm, as compared to previously reported values around 40 nm.^{7,8}

^{a)}Present Address: School of Electronic and Electrical Engineering, The University of Leeds, Woodhouse Lane, Leeds LS2 9JT, UK. Electronic mail: l.h.li@leeds.ac.uk.

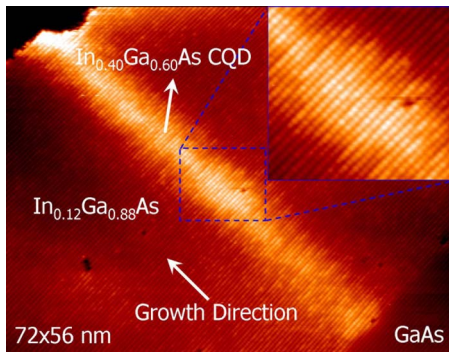


FIG. 1. (Color online) X-STM image of a CQD with $N=30$ periods (0.95 ML InAs/6 ML GaAs) SL. The measurement was performed in constant current mode with $V=-3.3$ V applied to the sample and current set at $I=32$ pA. The bright areas correspond to In-rich areas which have an outward relaxation proportional to the amount of In.

Cross sectional scanning tunneling microscopy (X-STM) has been performed at room temperature on the CQDs with $N=30$ periods (0.95 ML InAs/6 ML GaAs) SL. The STM is performed in the constant current mode on samples cleaved in the $[110]$ or $[1\bar{1}0]$ plane under ultrahigh vacuum conditions. The high applied voltages of around -3 V provide sensitivity to topographic distortions such as outward or inward relaxation, which in turn depend on the amount of strain and thus on the composition. Figure 1 presents one of the X-STM images, showing a rodlike structure which has a height of 69 ± 5 nm and a diameter of 11.2 ± 1.5 nm, close to the average diameter of seven measured CQDs. Assuming a uniform CQD composition and that the dot is cleaved through the center, we estimate a $x_{\text{CQD}}=40 \pm 5\%$ from the outward relaxation relative to that of the surrounding InGaAs. The x_{2D} of the InGaAs layer is estimated at $12 \pm 2\%$, in agreement with the value deduced by x-ray diffraction.

We investigated the polarization properties of CQDs with different aspect ratio and compositional contrast. Active regions comprising 3–5 CQD layers were embedded into P-i-N heterostructures with AlGaAs cladding layers, for waveguide and carrier confinement. The samples were processed into ridge-waveguide structures with 10–20 μm width. All measurements were taken at room temperature and electroluminescence (EL) was collected from the cleaved facet. Figure 2 shows the TE and TM integrated EL as a function of injection current, for the CQDs with (a) $N=18$ periods (0.7 ML InAs/3 ML GaAs) SL; and (b) $N=35$ periods (0.95 ML InAs/6 ML GaAs) SL. In the insets, typical transmission electron micrographs of the CQDs with corresponding SL structures are shown. A clear change in dominant polarization from TE to TM is observed upon changing the aspect ratio from 1.2 to ≈ 10 , and the average In composition x_{2D} from 16% to 12%. The prevailing TM-polarized emission in the $N=35$ sample clearly indicates a dominant light-hole character of the valence-band ground state. Detailed calculations^{18,19} show that the composition ratio x_{CQD}/x_{2D} is a key factor for the polarization control, and should be >3 to achieve a light-holelike ground state. The control of x_{2D} is thus essential.

To further demonstrate TM-polarized optical gain, we tested ridge-waveguide laser structures (3 mm \times 11 μm) under high injection. The active region is formed by three stacks of CQDs with a $N=35$ periods (0.95 ML InAs/6 ML

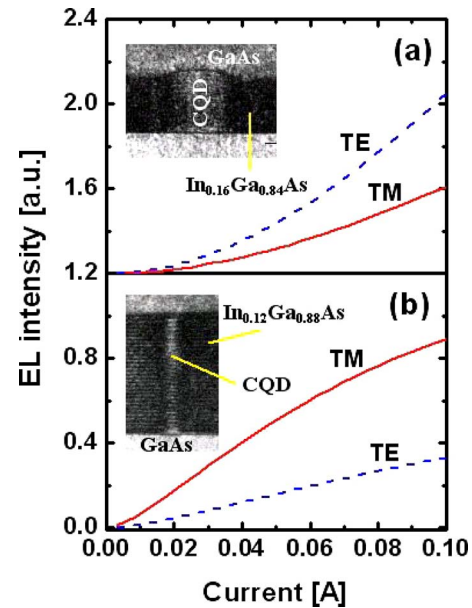


FIG. 2. (Color online) Normalized TE- and TM-polarized EL vs current from the facets of 2 mm long ridge-waveguides containing: (a) five stacks of CQDs with $N=18$ periods (0.7 ML InAs/3 ML GaAs) SL (ridge width: 23 μm); and (b) three stacks of CQDs with $N=35$ periods (0.95 ML InAs/6 ML GaAs) SL (ridge width: 19 μm). Insets: (a) TEM image of a CQD with $N=16$ periods (0.62 ML InAs/3 ML GaAs) SL; (b) TEM image of a CQD with $N=35$ periods (0.95 ML InAs/6 ML GaAs) SL.

GaAs) SL, separated by 100 nm thick GaAs spacer layers. The emission spectra measured just above threshold (at 1.1 kA/cm²) for the two polarizations are shown in Fig. 3, while the TM-polarized light-current curve is reported in the inset. The EL spectra are well distinct for TE and TM polarizations, with TM (TE) emission centered around 1190 (1140) nm. This confirms that the ground state transition involves valence band states with large light-hole component, while the states with large heavy-hole components are blue-shifted by ≈ 40 meV. A clear lasing peak is observed in TM polarization, at the peak of the TM amplified spontaneous emission spectra, while the much lower TE peak is due to the finite extinction ratio of the polarizer. The demonstration of TM lasing is a clear evidence of TM-dominant gain in these InAs/GaAs CQDs, which has never been reported before in compressive strain material systems.

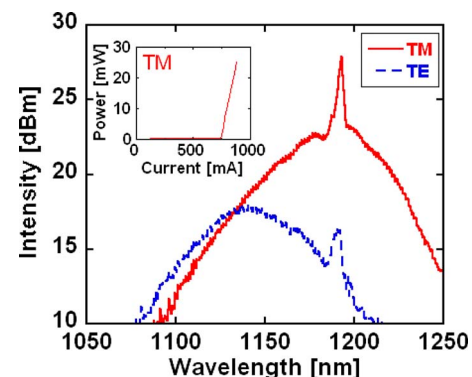


FIG. 3. (Color online) Lasing spectra in TE and TM polarizations for CQDs with $N=35$ periods SL (3 mm \times 11 μm). All samples have three stacks of CQDs spaced by 100 nm, and were measured at 20 $^{\circ}\text{C}$. Inset: TM-polarized light-current characteristics.

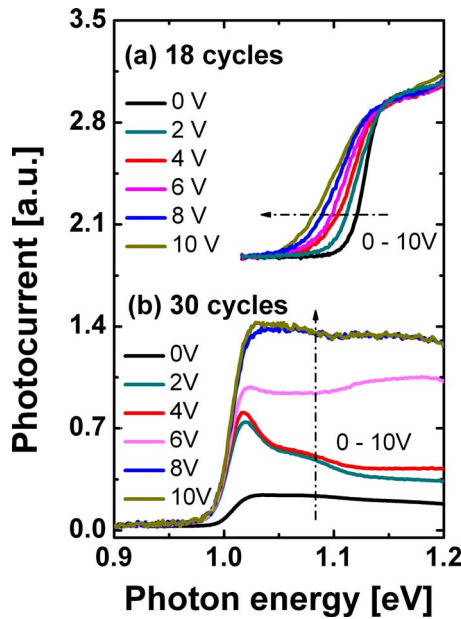


FIG. 4. (Color online) Room temperature photocurrent spectra at various reverse bias for CQDs with (a) $N=18$ and (b) $N=30$ periods SL.

We further investigated the dipole moment in different CQD structures by studying the quantum-confined stark effect (QCSE) by waveguide photocurrent spectroscopy under electric field. All measurements were taken at room temperature. For the lower aspect ratio CQD sample ($N=18$ periods) in Fig. 4(a), the photoabsorption edge is redshifted with increasing bias, the amplitude of the shift being enhanced as compared to that of a conventional QD.³ The number of states in a larger dot is greater while the spatial separation of electron and hole wave functions, determining their transition oscillator strength, change very rapidly with applied field as the electrons are spread out over the entire dot volume. The oscillator strength of the lowest energy transition is thus reduced with increasing field and the observed absorption becomes the result of higher-energy transitions, which explains the broadening of the absorption edge in Fig. 4(a). However, the sign of the shift is similar to the one observed in a conventional QD (redshift for an electric field pointing in the growth direction), indicating a positive dipole moment.⁵

In Fig. 4(b), we observe a strikingly different behavior for the larger aspect ratio CQD sample ($N=30$ periods). In this case, a clear excitonic peak is observed, whose amplitude peaks around 4 V. This behavior was also observed on other CQD structures with larger aspect ratios. The fact that the excitonic feature becomes stronger for increasing values of reverse bias is due to the enhancement of the overlap of the electron and hole envelope wave functions³ indicating a “mean” dipole moment value of different sign, i.e., negative, than that of the lower aspect ratio CQD. The energy shift of

the photoabsorption edge is in this case less apparent due to the varying amplitude of the excitonic absorption feature, preventing a direct extraction of the dipole moment value. The observed features clearly indicate that the sign and amplitude of the dipole moment can be controlled by the CQD aspect ratio, opening the way to its nanoscale engineering, with possible application to electro-optic modulators.

In conclusion, we have demonstrated how the combined control of shape and composition of semiconductor nanostructures can be used to manipulate their polarization and electro-optical properties. By varying the aspect ratio and compositional contrast between the CQD and its surrounding matrix, we have obtained TM-polarized lasing and changed the dipole moment in compressive strain material systems. This type of nanoscale engineering will be a key tool for practical applications of QDs.

We acknowledge financial support from the EU-FP6 Project ZODIAC (Contract No. FP6/017140) and the Swiss National Science Foundation.

- ¹K. L. Silverman, R. P. Mirin, S. T. Cundiff, and A. G. Norman, *Appl. Phys. Lett.* **82**, 4552 (2003).
- ²O. Stier, M. Grundmann, and D. Bimberg, *Phys. Rev. B* **59**, 5688 (1999).
- ³P. W. Fry, I. E. Itskevich, D. J. Mowbray, M. S. Skolnick, J. J. Finley, J. A. Barker, E. P. O'Reilly, L. R. Wilson, I. A. Larkin, P. A. Maksym, M. Hopkinson, M. Al-Khafaji, J. P. R. David, A. G. Cullis, G. Hill, and J. C. Clark, *Phys. Rev. Lett.* **84**, 733 (2000).
- ⁴P. Jin, C. M. Li, Z. Y. Zhang, F. Q. Liu, Y. H. Chen, X. L. Ye, B. Xu, and Z. G. Wang, *Appl. Phys. Lett.* **85**, 2791 (2004).
- ⁵K. Mukai, Y. Nakata, H. Shoji, M. Sugawara, K. Ohtsubo, N. Yokoyama, and H. Ishikawa, *Electron. Lett.* **34**, 1588 (1998).
- ⁶J. He, R. Notzel, P. Offermans, P. M. Koenraad, Q. Gong, G. J. Hamhuis, T. J. Eijkemans, and J. H. Wolter, *Appl. Phys. Lett.* **85**, 2771 (2004).
- ⁷J. He, H. J. Krenner, C. Pryor, J. P. Zhang, Y. Wu, D. G. Allen, C. M. Morris, M. S. Sherwin, and P. M. Petroff, *Nano Lett.* **7**, 802 (2007).
- ⁸L. H. Li, P. Ridha, G. Patriarche, N. Chauvin, and A. Fiore, *Appl. Phys. Lett.* **92**, 121102 (2008).
- ⁹L. H. Li, G. Patriarche, N. Chauvin, P. Ridha, M. Rossetti, J. Andrzejewski, G. Sek, J. Misiewicz, and A. Fiore, *IEEE J. Sel. Top. Quantum Electron.* **14**, 1204 (2008).
- ¹⁰J. T. Hu, L. S. Li, W. D. Yang, L. Manna, L. W. Wang, and A. P. Alivisatos, *Science* **292**, 2060 (2001).
- ¹¹S. Anantathanasarn, R. Notzel, P. J. van Veldhoven, F. W. M. van Otten, T. J. Eijkemans, and J. H. Wolter, *Appl. Phys. Lett.* **88**, 063105 (2006).
- ¹²T. Kita, O. Wada, H. Ebe, Y. Nakata, and M. Sugawara, *Jpn. J. Appl. Phys., Part 2* **41**, L1143 (2002).
- ¹³T. Kita, N. Tamura, O. Wada, M. Sugawara, Y. Nakata, H. Ebe, and Y. Arakawa, *Appl. Phys. Lett.* **88**, 211106 (2006).
- ¹⁴P. Ridha, L. H. Li, A. Fiore, G. Patriarche, M. Mexis, and P. M. Smowton, *Appl. Phys. Lett.* **91**, 191123 (2007).
- ¹⁵N. Yasuoka, K. Kawaguchi, H. Ebe, T. Akiyama, M. Ekawa, S. Tanaka, K. Morito, A. Uetake, M. Sugawara, and Y. Arakawa, *Appl. Phys. Lett.* **92**, 101108 (2008).
- ¹⁶H. J. Krenner, C. Pryor, J. He, J. P. Zhang, Y. Wu, C. M. Morris, M. S. Sherwin, and P. M. Petroff, *Physica E (Amsterdam)* **40**, 1785 (2008).
- ¹⁷L. H. Li, G. Patriarche, and A. Fiore, *J. Appl. Phys.* **104**, 113522 (2008).
- ¹⁸E. P. O'Reilly (private communication).
- ¹⁹P. Ridha, L. H. Li, M. Mexis, P. M. Smowton, J. Andrzejewski, G. Sek, J. Misiewicz, E. P. O'Reilly, G. Patriarche, and A. Fiore (unpublished).